25th ABCM International Congress of Mechanical Engineering
October 20-25, 2019, Uberlândia, MG, Brazil

COB-2019-2036
STABILITY ANALYSIS OF VISCOELASTIC FLUID FLOWS FOR HIGH WEISSENBERG NUMBERS

Laison Junio da Silva Furlan
Matheus Tozo de Araujo
Leandro Franco de Souza
Instituto de Ciências Matemáticas e de Computação, Universidade de São Paulo
Av. Trabalhador São Carlense, 400
13566-590, São Carlos, SP
laisonfurlan@gmail.com, matheustozo@gmail.com, lefraso@icmc.usp.br

Analice Costacurta Brandi
Faculdade de Ciências e Tecnologia, Universidade Estadual Paulista "Júlio de Mesquita Filho"
Rua Roberto Simonsen, 305
19060-900, Presidente Prudente, SP
analice.brandi@unesp.br

Márcio Teixeira de Mendonça
Instituto de Aeronáutica e Espaço, Divisão de Propulsão Aeronáutica - CTA/IAE/APA
Pç Marechal Eduardo Gomes, 50
12228-904, São José dos Campos, SP
marciomtm@fab.mil.br

Abstract. *Hydrodynamic instability has emerged as an active field of study in non-Newtonian fluid mechanics and their study and results are being increasingly explored. The flow of non-Newtonian fluids between parallel plates is a problem of considerable practical interest and this study will be considered. In this paper, the stability of the non-stationary disturbances of viscoelastic fluid is studied through the growth rate of Tollmien-Schlichting waves for incompressible two-dimensional fluid flow in a straight channel. The mathematical model adopted for the non-Newtonian fluid is the Giesekus model. The analysis is carried out by means of Direct Numerical Simulation (DNS) and Linear Stability Theory (LST). For the high Weissenberg number problem (HWNP), the Log-Conformation formulation was considered for the conformation tensor decomposition of the Giesekus model. In order to evaluate the maximum amplification rates and the neutral stability curves, different numerical simulations were performed by varying the non-dimensional parameters of the viscoelastic fluid flow.*
Keywords: *Straight channel, viscoelastic fluid flow, Log-Conformation formulation, Direct Numerical Simulation, Linear Stability Theory.*

1. INTRODUCTION

Viscoelastic fluids are complex fluids that describe many flows of industrial products, such as polymers, petroleum, food, cosmetics, and their study has been widely developed over the last decades. In the literature could be found many works about constitutive models of viscoelastic fluids, such as the differential models of Maxwell [Beris *et al.* (1987)], Oldroyd-B [Brasseur *et al.* (1994), Mompean and Deville (1997)], Giesekus [Giesekus (1962), Giesekus (1982)], models of FENE type [Bird *et al.* (1980)], PTT [Phan-Thien and Tanner (1977)]; and the integral models: Maxwell [Kaye (1962)] and K-BKZ [Luo and Tanner (1986), Luo and Tanner (1988)].

The process of a laminar flow becoming turbulent is known as laminar–turbulent transition [Schmid and Henningson (2001)]. This process is extremelly complex and actually is not complete established. Laminar flows are always subject to small disturbances. These disturbances appears by many factors, such that, structural vibrations, surface roughness, noise, external turbulence, etc. If these disturbances are not smoothed the laminar flow undergoes transition to another complex state, but not necessarily to turbulent state flow [Souza *et al.* (2005)]. The mechanisms and phenomena relationed with the disturbances growth in the laminar flows are called instability. The hidrodynamic stability theory investigates how these disturbances are amplified or smoothed and how the evolution of these disturbances are relationed with the transition phenomena for turbulent flow [Zhang *et al.* (2013)].

Despite the impetuous effort and remarkable progress in viscoelastics fluid flows simulation, some numerical instability problems have arisen with this advance. The High-Weissenberg number problem (HWNP) was the major obstacle in computational rheology since the early 1970s. This numerical phenomena that leads to instabilities and/or to not convergence of the solution even with different formulations or discretizations [Palhares Junior (2014)]. In order to improve this problem many treatments were developed. An idea gained prominence with the use of matrix decomposition, given by [Fattal and Kupferman (2004), Fattal and Kupferman (2005)], that proposed a new formulation for the constitutive equation of the conformation tensor using the matrix-logarithm of tensor. After these works, Afonso [Afonso *et al.* (2012)] presented an advantageous formulation in terms of precision and stability, called "Kernel-conformation" which generalizes the formulations, such that, log-conformation transformation, $root^k$-conformation transformation, etc.

In this work, the incompressible two-dimensional straight channel flow was considered in the numerical simulations for Giesekus fluid, in which high values of Weissenberg number were investigated. For the numerical simulations using the DNS technique the governing equations are written in a vorticity-velocity formulation and in the LST technique the objective is to solve the modified Orr-Sommerfeld equation for the viscoelastic Giesekus fluid [Brandi *et al.* (2019)]. The linear system arising from the numerical solution of the Poisson equation is solved by a multigrid methods. The Orr-Sommerfeld equation is solved by shooting method. The spatial derivatives are discretized by compact finite difference schemes [Lele (1992)] and the time integration is carried out by a fourth-order Runge-Kutta method [Souza (2003)]. The log-conformation formulation was used for the simulations considering high Weissenberg numbers. In order to evaluate the maximum amplification rates, different values of dimensionless parameters are tested for the Giesekus model.

2. MATHEMATICAL FORMULATION

In this paper, it is assumed a two-dimensional unsteady non-Newtonian fluid flow, incompressible and without body forces. The equations that describe this flow are the continuity and Navier-Stokes equations with a expression for the non-Newtonian extra-stress tensor, that in this paper is considered the Giesekus constitutive equation. These equations, in the dimensionless form, are given by

$$\nabla \cdot \mathbf{u} = 0, \tag{1}$$

$$\frac{\partial \mathbf{u}}{\partial t} + \nabla \cdot (\mathbf{uu}) = -\nabla p + \frac{\beta}{Re}\nabla^2 \mathbf{u} + \nabla \cdot \mathbf{T}, \tag{2}$$

where $\mathbf{u}$ denotes the velocity field, t is the time, p is the pressure and $\mathbf{T}$ is the extra-stress tensor. The dimensionless parameter $Re = (\rho UL)/(\eta)$ denotes the Reynolds number. The amount of Newtonian solvent is controlled by the dimensionless solvent viscosity coefficient, $\beta = \eta_s/\eta_0$, where $\eta_0 = \eta_s + \eta_p$ denotes the total shear viscosity; η_s and η_p represent the Newtonian solvent and polymeric viscosities, respectively. In this paper, we worked with viscoelastic flows governed by the non-linear Giesekus constitutive equation [Giesekus (1982)], given by

$$\mathbf{T} + Wi\,\overset{\nabla}{\mathbf{T}} + \frac{\alpha_G\, Wi\, Re}{(1-\beta)}(\mathbf{T}\cdot\mathbf{T}) = 2\frac{(1-\beta)}{Re}\mathbf{D}, \tag{3}$$

where $\mathbf{D} = \frac{1}{2}(\nabla\mathbf{u} + (\nabla\mathbf{u})^T)$ is the rate of deformation tensor, $Wi = (\lambda U)/(L)$ denotes the associated Weissenberg number, with λ representing the relaxation-time of the fluid, α_G is the so-called mobility parameter and $\overset{\nabla}{\mathbf{T}}$ is the upper-convected derivative of $\mathbf{T}$, defined by

$$\overset{\nabla}{\mathbf{T}} = \frac{\partial \mathbf{T}}{\partial t} + \nabla\cdot(\mathbf{uT}) - \mathbf{T}\cdot(\nabla\mathbf{u})^T - (\nabla\mathbf{u})\cdot\mathbf{T}. \tag{4}$$

2.1 Log-Conformation Method

The Log-conformation method [Fattal and Kupferman (2004)] proposes a reformulation of the constitutive equation of the tensor in order to control the numerical instabilities caused by HWNP [Keunings (1986)].

The application of this method starts from two main steps: a decomposition applied to the tensor $\nabla\mathbf{u}$ and, later, a logarithmic transformation in $\mathbf{A}$, constructing a new constitutive equation for the logarithmic variable used. The polymeric contribution constitutive equation is frequently formulated in terms of the conformation tensor $\mathbf{A} = \mathbf{A}(\mathbf{x}, t)$, which is an approximation of microstructural state of liquid. Hulsen [Hulsen (1990)] has proved that the tensor conformation must remain SPD (symmetric positive definite) throughout the temporal evolution of the constitutive equation if it is initialized in this way, i.e. if was initialized SPD.

The equation that relates the conformation tensor $\boldsymbol{A}$ to the polymeric contribution $\boldsymbol{\tau}$ is equation (5). This relationship between tensors varies according to the chosen constitutive model. For the Giesekus model, this relation is given by

$$\boldsymbol{\tau} = \boldsymbol{\xi}(\boldsymbol{A} - \boldsymbol{I}), \tag{5}$$

where $\xi = \dfrac{1-\beta}{ReWi}$.

The constitutive equation of the conformation tensor $\mathbf{A}$ is given by

$$\frac{\partial \boldsymbol{A}}{\partial t} + (\boldsymbol{u}\cdot\nabla)\boldsymbol{A} - (\boldsymbol{\Omega A} - \boldsymbol{A\Omega}) - 2\boldsymbol{BA} = \frac{1}{Wi}M(\boldsymbol{A}), \tag{6}$$

where $M(\mathbf{A})$ is defined according to the viscoelastic model. For Giesekus model, $M(\mathbf{A}) = (\mathbf{I}-\mathbf{A})[\mathbf{I}+\alpha_G(\mathbf{A}-\mathbf{I})]$.

Thus, we define the logarithm of the conformation tensor as

$$\Psi = \log_a(\mathbf{A}) = \mathbf{O}\log_a(\mathbf{\Lambda})\mathbf{O}^T, \tag{7}$$

which implies, by inverse property, in

$$a^{\Psi} = \mathbf{A}. \tag{8}$$

Therefore, the log-conformation formulation equation can be written as

$$\frac{\partial \mathbf{\Psi}}{\partial t} + \nabla\cdot(\mathbf{u\Psi}) = (\mathbf{\Omega\Psi} - \mathbf{\Psi\Omega}) + 2\mathbf{B} + \frac{1}{Wi}a^{-\mathbf{\Psi}}(\mathbf{I}-a^{\mathbf{\Psi}})[\mathbf{I}+\alpha_G(a^{\mathbf{\Psi}}-\mathbf{I})]. \tag{9}$$

In practice, it is adopted $a = e$ (natural logarithm).

2.2 Direct Numerical Simulation

In this paper, we employ high order finite difference schemes, such that all flow scales are simulated, from the largest and most energetic to the smallest, without adding closing equations.

In order to eliminate the pressure term in the Navier-Stokes equations, it is adopted the vorticity-velocity formulation. Thus, the vorticity in direction z, ω_z, is defined by

$$\omega_z = \frac{\partial u}{\partial y} - \frac{\partial v}{\partial x}. \tag{10}$$

Therefore, the equations (1)-(3) in the two-dimensional can be rewritten as

$$\frac{\partial u}{\partial x} + \frac{\partial v}{\partial y} = 0, \tag{11}$$

$$\frac{\partial^2 v}{\partial x^2} + \frac{\partial^2 v}{\partial y^2} = -\frac{\partial \omega_z}{\partial x}, \tag{12}$$

$$\frac{\partial \omega_z}{\partial t} + \frac{\partial (u\omega_z)}{\partial x} + \frac{\partial (v\omega_z)}{\partial y} = \frac{\beta}{Re}\left(\frac{\partial^2\omega_z}{\partial x^2} + \frac{\partial^2\omega_z}{\partial y^2}\right) + \frac{\partial^2 T^{xx}}{\partial x\partial y} + \frac{\partial^2 T^{xy}}{\partial y^2} - \frac{\partial^2 T^{xy}}{\partial x^2} - \frac{\partial^2 T^{yy}}{\partial x\partial y}, \tag{13}$$

$$T^{xx} + Wi\Big(\frac{\partial T^{xx}}{\partial t} + \frac{\partial (uT^{xx})}{\partial x} + \frac{\partial (vT^{xx})}{\partial y} - 2T^{xx}\frac{\partial u}{\partial x} - 2T^{xy}\frac{\partial u}{\partial y}\Big) + \alpha_G\frac{WiRe}{(1-\beta)}(T^{xx^2} + T^{xy^2}) = \\ = 2\frac{(1-\beta)}{Re}\frac{\partial u}{\partial x}, \tag{14}$$

$$T^{xy} + Wi\Big(\frac{\partial T^{xy}}{\partial t} + \frac{\partial (uT^{xy})}{\partial x} + \frac{\partial (vT^{xy})}{\partial y} - T^{xx}\frac{\partial v}{\partial x} - T^{yy}\frac{\partial u}{\partial y}\Big) + \alpha_G\frac{WiRe}{(1-\beta)}(T^{xx}T^{xy} + T^{xy}T^{yy}) = \\ = \frac{(1-\beta)}{Re}\Big(\frac{\partial v}{\partial x} + \frac{\partial u}{\partial y}\Big), \tag{15}$$

$$T^{yy} + Wi\Big(\frac{\partial T^{yy}}{\partial t} + \frac{\partial (uT^{yy})}{\partial x} + \frac{\partial (vT^{yy})}{\partial y} - 2T^{xy}\frac{\partial v}{\partial x} - 2T^{yy}\frac{\partial v}{\partial y}\Big) + \alpha_G\frac{WiRe}{(1-\beta)}(T^{xy^2} + T^{yy^2}) = \\ = 2\frac{(1-\beta)}{Re}\frac{\partial v}{\partial y}. \tag{16}$$

In the computational domain, represented in Fig. 1, there are three types of boundary conditions adopted: inflow, outflow and wall boundary conditions. The inflow is specified according to the following conditions:

$$u = U(y), \quad v = 0, \quad \text{and} \quad \mathbf{T} = 0. \tag{17}$$

On wall boundaries, the no-slip condition and impermeability $(u = 0, v = 0)$ are employed. At the outflow the second derivative of variables in respect to x are set to zero.

2.2.1 Numerical Method

The system of equations considered in the DNS technique is solved numerically in the domain as shown in Fig. 1. The calculations are performed on an orthogonal uniform grid, parallel to the wall. The fluid enters the computational domain at $x = x_0$ and exits at the outflow boundary $x = x_{max}$.

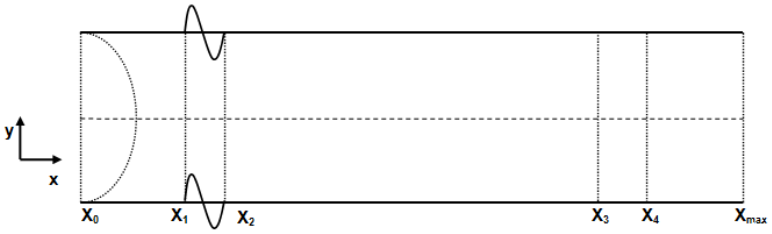

Figure 1. Definition of the computational domain for Poiseuille flow.

The flow variables for time $t = 0$, are undisturbed, therefore from time $t > 0$, the disturbances are introduced in a disturbance strip near the inflow (in both walls), through the imposition of the v velocity, given by

$$v = A\, f(x)\, sin(\omega_t\, t), \quad x_1 < x < x_2, \quad \text{and} \quad v = 0, \quad x \leq x_1 \quad \text{or} \quad x \geq x_2, \tag{18}$$

where A is a constant used to adjust the amplitude of the disturbances, $f(x)$ is a 9th-order function and ω_t is the disturbance temporal frequency. The points x_1 and x_2 are the initial and the last point of the disturbance strip, respectively. The values of $f(x)$, its first, and second derivatives are zero in these extreme points. To avoid wave reflections from the inflow and outflow boundaries, it was implemented a buffer domain technique, from (Kloker *et al.*, 1993), in the region located between x_0 and x_1 and x_3 and x_4, respectively. The simulation finishes when a periodic flow is reached and the disturbances reach the region close to the end of the domain in the streamwise position.

2.3 Linear Stability Theory

The LST technique consider that the flow can be decomposed in a base flow and a disturbed flow. These disturbances can be written in the general form as

$$\tilde{\mathbf{u}} = \overline{\mathbf{u}}(y)e^{i(\alpha x - \omega t)}, \quad \tilde{p} = \overline{p}(y)e^{i(\alpha x - \omega t)}, \quad \tilde{\mathbf{T}} = \overline{\mathbf{T}}(y)e^{i(\alpha x - \omega t)}, \tag{19}$$

where, considering two-dimensional flow $\tilde{\mathbf{u}} = (\tilde{u}, \tilde{v})$, $\overline{\mathbf{u}} = (\overline{u}, \overline{v})$, $\tilde{\mathbf{T}} = (\tilde{T}_{xx}, \tilde{T}_{xy}, \tilde{T}_{yy})$ and $\overline{\mathbf{T}} = (\overline{T}_{xx}, \overline{T}_{xy}, \overline{T}_{yy})$.

The autofunctions $\tilde{u}, \tilde{v}, ..., \tilde{T^{yy}}$ can be complex functions of y. The wave length of the disturbances in the streamwise direction (x) is denoted for the complex parameter α, which shows the disturbances propagation along the flow in the streamwise direction and if these disturbances are stable, unstable or neutral.

The LST technique has objective the solution of the Orr-Sommerfeld equation (20). For a viscoelastic fluid, the Orr-Sommerfeld equation is modified and solved for this model. The solution correspond a eigenvalue problem whose solution exists for some parameter values $\alpha, \omega, Re, Wi, \beta$, and depends the velocity profile of the base flow.

The Orr-Sommerfeld equation modified for a viscoelastic fluid considering a two-dimensional problem is given by

$$\alpha(U-c)\left(\frac{d^2\overline{v}}{dy^2} - \alpha^2\overline{v}\right) - \alpha\overline{v}\frac{d^2U}{dy^2} + \alpha\frac{d^2\overline{T}^{xy}}{dy^2} + i\alpha^2\left(\frac{d\overline{T}^{xx}}{dy} - \frac{d\overline{T}^{yy}}{dy}\right) + \alpha^3\overline{T}^{xy} = -\frac{i\beta}{Re}\left(\frac{d^4\overline{v}}{dy^4} - 2\alpha^2\frac{d^2\overline{v}}{dy^2} + \alpha^4\overline{v}\right). \tag{20}$$

The stability analysis is performed by studying the numerical solution of this equation and by the temporal and spatial stability diagrams constructed as the Table 1 shows.

2.3.1 Numerical Method

In LST technique the objective is solve the Orr-Sommerfeld equation (20) modified for a viscoelastic fluid. The solution of the modified Orr-Sommerfeld equation corresponds to an eigenvalue problem, whose solution is linked to the parameter values $\alpha, \omega, Re, \beta, \alpha_G$ and Wi, and depends on the base flow velocity profile.

The computational process was performed by [Mendonça and de Medeiros (2002)] adopting the Shooting method to solve the Orr-Sommerfeld equation for a non-Newtonian fluid of Giesekus type.

- Consider the initial values for the eigenvalues $\alpha, \omega, Re, Wi, \alpha_G$ and β;

Table 1. Instabilities classification.

Type of analysis	Amplification rate	Amplitude	Classification
Temporal analysis	$\omega_i < 0$	decreases	stable
	$\omega_i = 0$	constant	neutral
	$\omega_i > 0$	increase	unstable
Spatial analysis	$\alpha_i < 0$	increase	unstable
	$\alpha_i = 0$	constant	neutral
	$\alpha_i > 0$	decreases	stable

- Integrate the Orr-Sommerfeld equation by 4th order Runge-Kutta scheme starting from the lower boundary;
- Verify if the boundary condition at the upper boundary is satisfied;
- Change the value of ω (or α depending on the analysis - temporal or spatial) and integrates again te Orr-Sommerfeld equation;
- Verify if the boundary condition on the wall is satisfied;
- If the checked condition is not satisfied, it interpolates ω through the last two approaches.

3. CODE VERIFICATION

In order to verify the DNS and the LST code implemented with the Giesekus fluid and the log-conformation transformation, we consider two-dimensional fluid flow between parallel plates. Numerical simulations were performed in order to compare the base flow generated numerically with the DNS code implemented with the Giesekus model, considering $\alpha_G = 0$ in mathematical model and comparing with the base flow generated analytically with the DNS code implemented with the Oldroyd-B model.

For verification test of implemented code, the following parameters were adopted: the number of points in the streamwise and wall-normal directions are $i_{max} = 9049$ and $j_{max} = 249$, respectively; the distance between two consecutive points in the x- and y-directions are $dx = 2\pi/(32\alpha_r)$ and $dy = 2/(jmax - 1)$, respectively, where α_r is the real part of the wavenumber; the time steps per wave period is 128.

Figure 2 shows the comparison between the analytical solution of Oldroyd-B fluid and the numerical solution obtained using a DNS technique for Giesekus fluid considering $\alpha_G = 0$. In this figure was performed three simulations, considering $Re = 2000, 5000$ and 8000, $\beta = 0.25, 0.50$ and 0.75 and $Wi = 10, 15$ and 20.

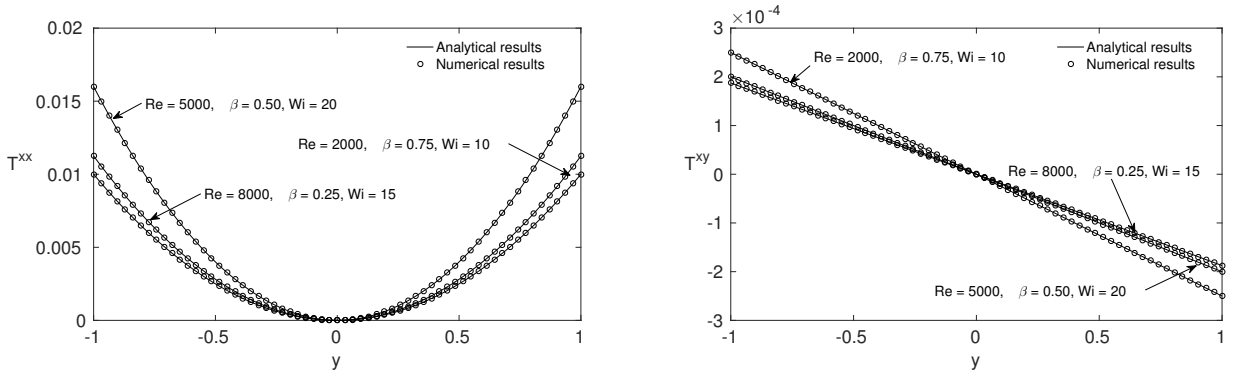

Figure 2. Comparison between the analytical solution of Oldroyd-B fluid and the numerical solution obtained using a DNS technique.

It can be seen the analytical and the numerical solutions are in agreement for the three simulations performed. Figure 3 shows the error between analytical solution and numerical solution and it can be noted that the error grows when the dx is increasily and the convergence order of error is approximately 10^{-5}.

4. NUMERICAL RESULTS

Different numerical simulations were performed by varying the non-dimensional parameters for the viscoelastic Giesekus fluid, in order to evaluate the maximum amplification rates. In these simulations the following parameters

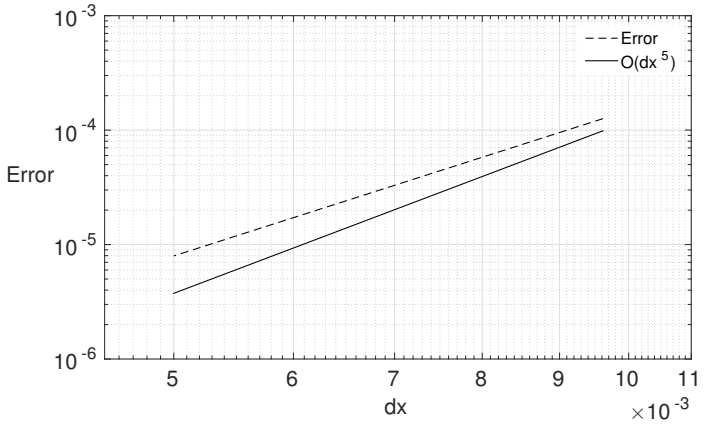

Figure 3. Error between analytical and numerical solutions.

were considered: $Re = 2000, 3000, 4000, 5000, 6000, 7000$ and 8000, $\beta = 0.75$ and 0.90, $\alpha_G = 0.1, 0.2$ and 0.3, $Wi = 1, 2, 5, 10, 25, 50, 75$ and 100.

The parameters adopted in DNS simulations carried out here were: the number of points in the streamwise and wall-normal directions are $i_{max} = 961$ and $j_{max} = 249$, respectively; the distance between two consecutive points in the x- and y-directions are $dx = 2\pi/(32\alpha_r)$ and $dy = 2/(jmax - 1)$, respectively, where α_r is the real part of the wavenumber.

4.1 Base Flow

In order to show the influence of Weissenberg number in the behavior of the Giesekus fluid flow components, some simulations were performed for the base flow with different values of Weissenberg number. The parameters adopted were: $Re = 4000,\ \beta = 0.75,\ \alpha_G = 0.30$ and $Wi = 1, 10, 100$.

Figure 4 shows the components profile $U(y)$ (velocity) and T^{xx}, T^{xy} and T^{yy} (non-Newtonian tensors) of the viscoelastic flow. It can be seen that in the velocity profile the velocity increases when Wi is increased. For the non-Newtonian tensors the opposite occurs, that is, the absolut value of the tensors component decreases when Wi is increased.

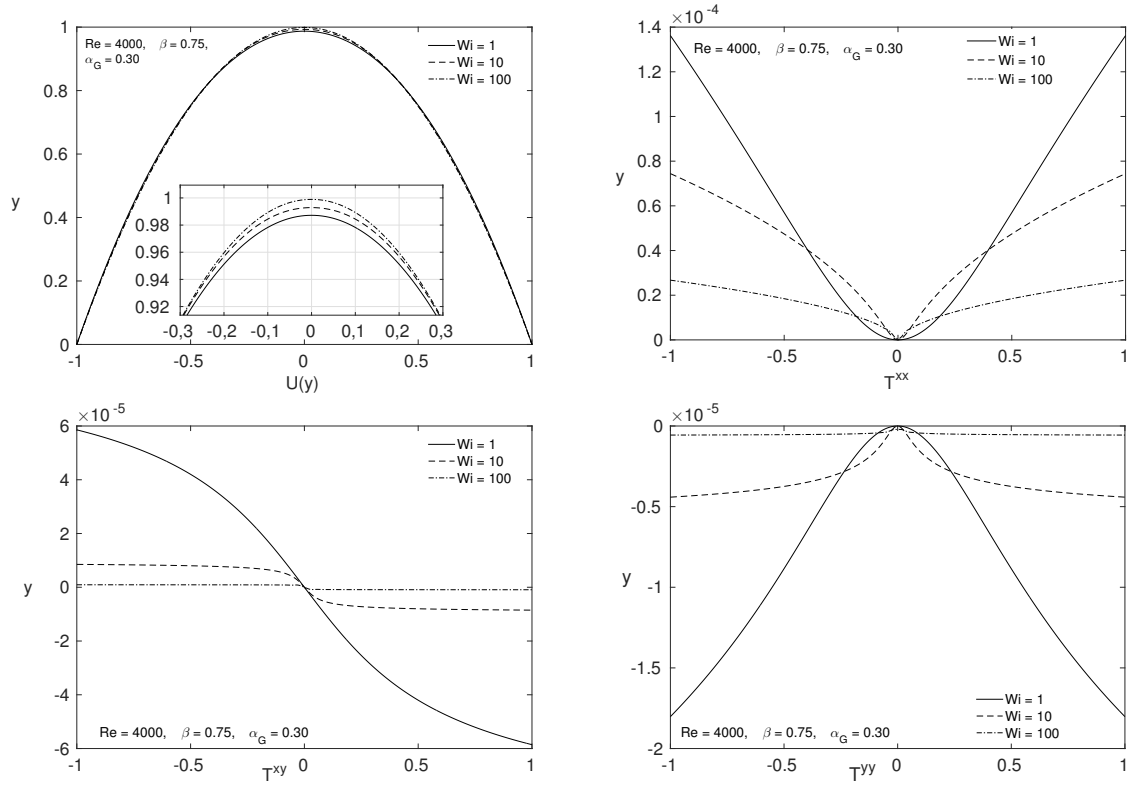

Figure 4. Components of viscoelastic fluid flow for different values of Weissenberg number.

4.2 Stability Analysis

In this section, the stability analysis of the Giesekus fluid flows were performed carried out by means DNS and LST techniques. In the DNS simulations were adopted the following parameters: 128 time steps per wave period, disturbance frequency $\omega_t = 0.2$ and the parameter A to adjust the amplitude of the Tollmien-Schlichting waves was 1×10^{-4}.

For LST technique numerical simulations were performed to find the spatial amplification rates values (α_i) for different Reynolds and ω_t values in order to determine the neutral curve, that is, where the values of $\alpha_i = 0$. In this diagram, the amplification rates smaller than zero $\alpha_i < 0$ (unstable) are inside the curve and the amplification rates greater than zero $\alpha_i > 0$ (stable) are outside the curve.

In order to verify the results obtained using both techniques, different numerical simulations were performed by varying the Weissenberg number for Giesekus fluid flows and their results were compared as can be seen in Fig. 5.

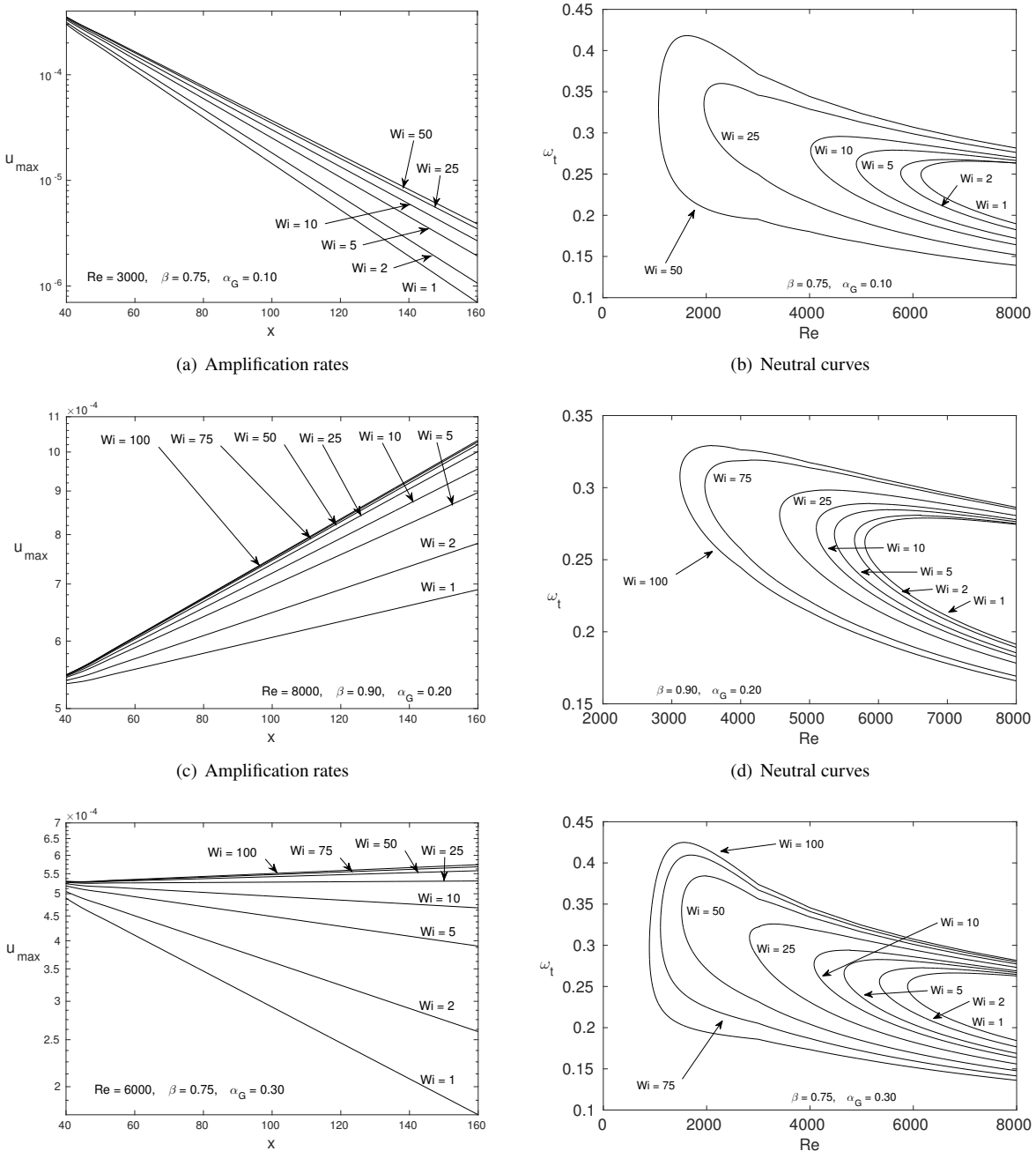

(a) Amplification rates

(b) Neutral curves

(c) Amplification rates

(d) Neutral curves

(e) Amplification rates

(f) Neutral curves

Figure 5. Comparison between DNS and LST results.

Figure 5(a) shows that for all Wi numbers performed the flow is still stable even when Wi is increased. This conclusion can be verified by the neutral curves presented in Fig. 5(b). In Figure 5(c) it can be noted that for all Wi numbers

performed the flow is still unstable even when Wi is decreased and this can be verified by the neutral curves presented in Fig. 5(d). Figure 5(e) shows that the flow will be stable for $Wi = 1, 2, 5$ and 10, unstable for $Wi = 50, 75$ and 100, and neutral for $Wi = 25$ as can be seen in neutral curves presented in Fig. 5(f).

Figure 6 shows neutral curves obtained by LST technique varying Wi number and different dimensionless parameters. In all neutral curves presented it can be seen that the instability region grows when Wi is increased.

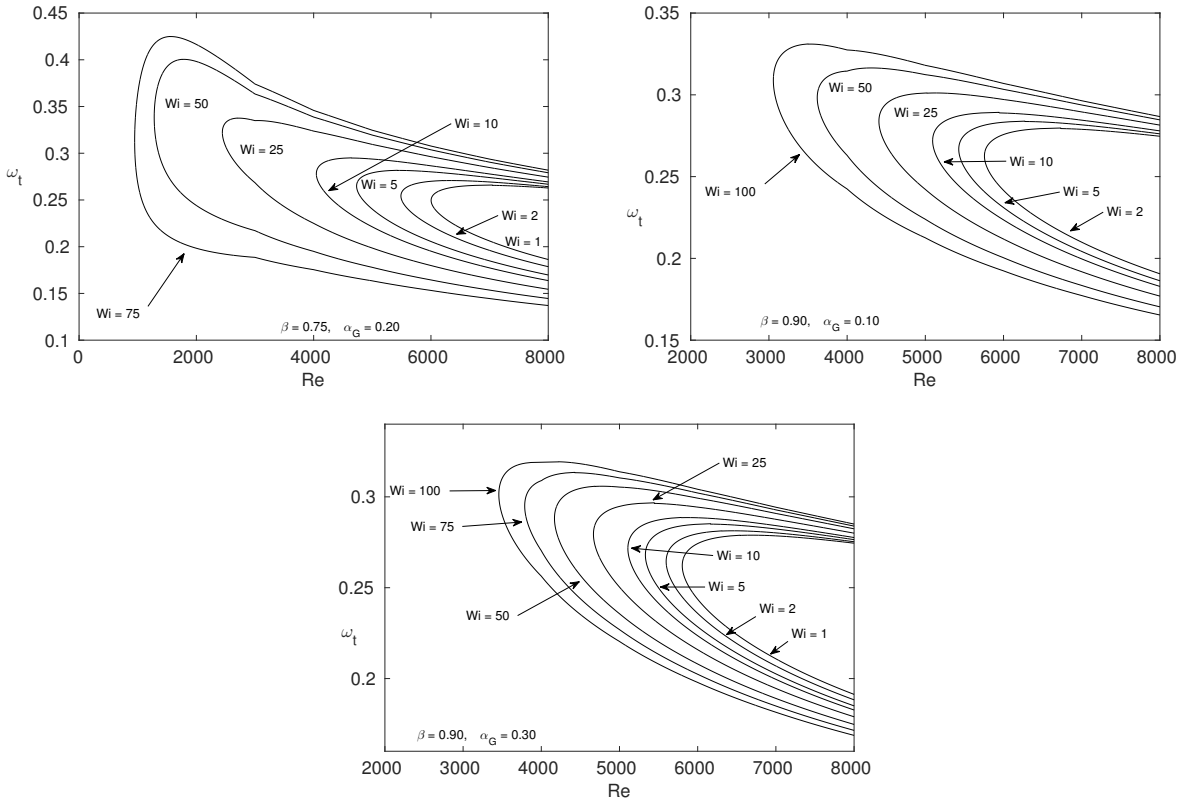

Figure 6. Neutral curves of instability.

5. CONCLUSION

The present paper shows two techniques to investigate the stability of the viscoelastic fluid flow in a straight channel, Linear Stability Theory and Direct Numerical Simulation. It was considered the Giesekus constitutive equation for the numerical simulation with the implementation of the Log-Conformation formulation to solve the high Weissenberg number problem. In order to evaluate the maximum amplification rates for different Reynolds and Weissenberg values, different values of these dimensionless parameters are tested.

In order to verify the implemented code, some numerical simulations were performed for the Giesekus fluid flow considering $\alpha_G = 0$ and compared with the analytical solution of Oldroyd-B fluid flow. In addition, different values of Weissenberg number were performed with the objective to analyse the components behavior in the flow when Wi is increased.

The stability analysis were performed carried out by means DNS and LST techniques. The comparison between both techniques was accomplished in order to verify the consistence and agreement of the results obtained. The results show that when Wi number is increased the fluid flow becomes unstable for lower values of Reynolds number.

6. ACKNOWLEDGEMENTS

The authors acknowledge CAPES. Research carried out using the computational resource of the Center for Mathematical Applied to Industry (CeMEAI) funded by FAPESP (Process Number 2013/07375-0).

7. REFERENCES

Afonso, A.M., Pinho, F.T. and Alves, M.A., 2012. "The kernel-conformation constitutive laws". *Journal of Non-Newtonian Fluid Mechanics*, Vol. 167, pp. 30 – 37.

Beris, A., Armostrong, R. and Brown, R., 1987. "Spectral finite-element calculations of the flow of a Maxwell fluid between excetric rotating cylinders". *Journal of Non-Newtonian Fluid Mechanics*, Vol. 22, pp. 129–167.

Bird, R.B., Dotson, P.J. and Johnson, N.L., 1980. "Polymer solution rheology based on a finitely extensible bead-spring chain model". *Journal of Non-Newtonian Fluid Mechanics*, Vol. 7, pp. 213–235.

Brandi, A.C., Mendonça, M.T. and Souza, L.F., 2019. "Dns and lst stability analysis of oldroyd-b fluid in a flow between two parallel plates". *Journal of Non-Newtonian Fluid Mechanics*, Vol. 267, pp. 14 – 27.

Brasseur, E., Fyrillas, M., Georgioou, G. and Crochet, M., 1994. "The time-dependent extrudate-swell problem of an Oldroyd-B fluid with slip along the wall". *Journal of Rheology*, Vol. 42, pp. 549–566.

Fattal, R. and Kupferman, R., 2004. "Constitutive laws for the matrix-logarithm of the conformation tensor". *Journal of Non-Newtonian Fluid Mechanics*, Vol. 123, pp. 281 – 285.

Fattal, R. and Kupferman, R., 2005. "Time-dependent simulation of viscoelastic flows at high Weissenberg number using the log-conformation representation". *Journal of Non-Newtonian Fluid Mechanics*, Vol. 126, pp. 23 – 37.

Giesekus, H., 1962. "Elasto-viskose flüssigkeiten, für die in stationären schichtströmungen sämtliche normalspannungskomponenten verschieden gross sind". *Rheologica Acta*, Vol. 2, pp. 50–62.

Giesekus, H., 1982. "A simple constitutive equation for polymer fluids based on the concept of deformation-dependent tensorial mobility". *Journal of Non-Newtonian Fluid Mechanics*, Vol. 11, pp. 69–109.

Hulsen, M.A., 1990. "A sufficient condition for a positive definite configuration tensor in differential models". *Journal of Non-Newtonian Fluid Mechanics*, Vol. 38, pp. 93 – 100.

Kaye, A., 1962. *Non-newtonian flow in incompressible flows*. College of Aeronautics.

Keunings, R., 1986. "On the high weissenberg number problem". *Journal of Non-Newtonian Fluid Mechanics*, Vol. 20, pp. 209 – 226.

Kloker, M., Konzelmann, U. and Fasel, H.F., 1993. "Outflow boundary conditions for spatial navier-stokes simulations of transition boundary layers". *AIAA Journal*, Vol. **31**, pp. 620–628.

Lele, S., 1992. "Compact finite difference schemes with spectral-like resolution". *J. Comput. Phys.*, Vol. **103**, pp. 16–42.

Luo, X.L. and Tanner, R.I., 1986. "A streamline element scheme for solving viscoelastic flow problems part ii: Integral constitutive models". *Journal of Non-Newtonian Fluid Mechanics*, Vol. 22, pp. 61–89.

Luo, X.L. and Tanner, R.I., 1988. "Finite element simulation of long and short circlar die extrusion experiments using integral models". *International Journal for Numerical Methods in Engineering*, Vol. 25, pp. 9–22.

Mendonça, M.T. and de Medeiros, M.A.F., 2002. *Instabilidade Hidrodinâmica e transição para turbulência com aplicações em engenharia e meteorologia*. ENCIT - 2002.

Mompean, G. and Deville, M., 1997. "Unsteady finite volume of Oldroyd-B fluid through a three-dimensional planar contraction". *Journal of Non-Newtonian Fluid Mechanics*, Vol. 72, pp. 253–279.

Palhares Junior, I.L., 2014. *Decomposições matriciais para escoamentos viscoelásticos incompressíveis*. Master's thesis, Universidade Estadual Paulista "Julio de Mesquita Filho".

Phan-Thien, N. and Tanner, R.I., 1977. "A new constitutive equation derived from network theory". *Journal of Non-Newtonian Fluid Mechanics*, Vol. 2, pp. 353–365.

Schmid, P.J. and Henningson, D.S., 2001. *Stability and Transition in Shear Flows*. Springer.

Souza, L.F., 2003. *Instabilidade Centrífuga e transição para turbulência em Escoamentos Laminares Sobre Superfícies Côncavas*. Ph.D. thesis, Instituto Tecnológico de Aeronáutica.

Souza, L.F., Mendonça, M.T. and Medeiros, M.A.F., 2005. "The advantages of using high-order finite differences schemes in laminar-turbulent transition studies". *International Journal for Numerical Methods in Fluids*, Vol. **48**, pp. 565–592.

Zhang, M., Lashgari, I., Zaki, T.A. and Brandt, L., 2013. "Linear stability analysis of channel flow of viscoelastic Oldroyd-B and FENE-P fluids". *Journal of Fluid Mechanics*, Vol. 737, pp. 249–279.

8. RESPONSIBILITY NOTICE

The authors are the only responsible for the printed material included in this paper.